Mem. Fac. Eng., Kyoto Univ. Vol. 52, No. 4 (1990)

Heavy-Ion Rutherford Backscattering Spectrometry — A Comparison of ^{11}B with ^{4}He Ions —

by

Koji IWASAWA*, Gyo SATO*, Manabu SAITO*, Koji YOSHIDA*
Nobutsugu IMANISHI* and Fumio FUKUZAWA*

(Received June 28, 1990)

Abstract

The Rutherford backscattering spectrometry was examined with ^{11}B and ^{4}He ions. Backscattering spectra improve in the mass resolution, the depth resolution and the channeling minimum yield when 6 MeV ^{11}B ions are used instead of 2 MeV ^{4}He ions, which have been used commonly. Then the terminal voltage of a 1.7 MV tandem Cockcroft-Walton accelerator was calibrated by means of a combination of the $^{27}Al(p, \gamma)^{28}Si$ resonance method and a new iterative method using ^{1}H and ^{4}He ions. The true terminal voltage of the accelerator is lower than the corresponding nominal values, and the deviation quadratically increases with increasing voltage.

1. Introduction

The Rutherford backscattering spectrometry (RBS) is a very powerful method to analyze surfaces and thin films, and has been applied to various fields of technology. ^{4}He ions have been commonly used for the purpose by the following reasons:

1. ^{4}He ions can be extracted easily from single-ended electrostatic accelerators, which are widely used in many laboratories.
2. Data of stopping cross sections of ^{4}He in matters which are essential for the analysis of depth profiles, are more fertile than those of other ions.

However, ^{4}He ions are rather insufficient for the elemental analysis and the depth profile measurement of complicated materials, for which demand is increasing rapidly. Figures of merit of the Rutherford backscattering spectrometry, such as the sensitivity, the mass resolution, the depth resolution and the channeling minimum yield, depend on the atomic number, the atomic mass and the energy of an incident ion. It is expected that heavier ions can give better figures of merit unless an energy resolution of a silicon surface-barrier detector (SSD) deteriorates for heavy ions. Systematic studies are few

* Department of Nuclear Engineering

about the application of heavy ions to the Rutherford backscattering spectrometry[1)~4)]. Hence, we studied the figures of merit for 2-6 MeV ^{11}B ions in the Rutherford backscattering spectrometry and compared them with those for 1-4 MeV ^{4}He.

2. Experimental

2. 1 Ion beams

Experiments were carried out with a 1.7 MV Tandem Cockcroft-Walton accelerator (TANDETRON) system equipped with a goniometer system. The system has two ion sources, a duoplasmatron and a cesium-sputtering ion source. ^{4}He ions were extracted as $^{4}He^{+}$ ions from the former one at an energy of 20 keV, changed to negatively charged (1−) ions, and accelerated from the ground to the high voltage terminal. Then, their charge was changed to 2+ with Ar stripper gas and re-accelerated to the other ground. ^{1}H and ^{11}B ions were extracted as $^{1}H^{-}$ and $^{11}B^{-}$ ions from the latter one at an energy of 24 keV, and accelerated to the terminal. Then, their charges were changed to 1+ and 3+ for ^{1}H and ^{11}B ions, respectively, which were accelerated again.

2. 2 Calibration of terminal voltage

It is necessary to know the exact energy of an incident ion beam in order to analyze samples in detail with the Rutherford backscattering spectrometry. Therefore, we calibrated the terminal voltage of TANDETRON beforehand.

Resonance peaks[5)] of the $^{27}Al(p, \gamma)^{28}Si$ reaction at 632.23, 991.88 and 1213.08 keV have been commonly used for the calibration of the terminal voltage of an electrostatic accelerator. Resonance peaks above 1213.08 keV have, however, large uncertainties in their energies. Therefore, the "resonance method" is applicable in the voltage range below 0.6 MV, corresponding to the 1213.08 keV peak. Thus we have developed an alternative method to calibrate the terminal voltage above 0.6 MV.

First, an aluminum foil (99.99% pure, 20 μm thick) was used as a target of the "resonance method". Yield-curves of gamma-rays from the $^{27}Al(p, \gamma)^{28}Si$ reaction, which were taken with a 15 cmϕ × 10 cm NaI(Tl) scintillation detector, gave true terminal voltages corresponding to the above three resonance energies.

^{4}He ions were then accelerated at one of the above three terminal voltages and the backscattering spectra of $^{4}He^{2+}$ ions from a thin Au target were taken with a silicon surface-barrier detector which was set at an angle of 168.6° and had a Au window 40 $\mu m / cm^2$ thick. The target was prepared by a vacuum evaporation method on a Si single-crystal wafer of 10 mm × 10 mm area, and its thickness was measured as 5 nm thick with a crystal oscillator. Again, $^{1}H^{+}$ ions were accelerated and the terminal voltage V_H was adjusted to give the same energy as $^{4}He^{2+}$ ions by comparing the backscat-

tering spectrometry spectra of $^1H^+$ and $^4He^{2+}$ ions. Then, the following relations are obtained:

$$E_H = 2V_H + 24 \quad [\text{keV}] \tag{1}$$
$$E_{He} = 3V_{He} + 20 \quad [\text{keV}] \tag{2}$$
$$E_H = E_{He} \quad [\text{keV}] \tag{3}$$
$$V_H = 1.5V_{He} - 2 \quad [\text{kV}] \tag{4}$$

where, E_H and E_{He} are the energies of $^1H^+$ and $^4He^{2+}$ ions, respectively, and V_H and V_{He} are the true terminal voltages for the acceleration of $^1H^+$ and $^4He^{2+}$, respectively. A factor 1.5 is applied because of the charge difference between $^4He^{2+}$ and $^1H^+$, and a term -2 kV compensates the difference between the extraction voltages of the duoplasmatron and the cesium-sputtering ion source. As the voltage V_{He} was measured by the "resonance method" as described before, we could obtain the exact value of V_H from Eq. (4). In this way, $^4He^{2+}$ and $^1H^+$ ions were accelerated alternately and their backscattering spectra were taken. Thus, the true terminal voltages were fixed iteratively up to a maximum nominal terminal voltage of 1.7 MV. We will call this method as the "RBS-iterative method" hereafter.

In order to ensure that the $^1H^+$ ions accelerated at the same energy as $^4He^{2+}$ ions, the following procedure was taken. The terminal voltage was adjusted, first, for the channel number of the peak in the $^1H^+$ backscattering spectrum to agree with that of $^4He^{2+}$ ions. The peak channels were determined by fitting to Gaussian curves with the least squares method. Then, small corrections of K-factors, energy losses in the Au target and in the window of the detector were made.

2. 3 Rutherford backscattering spectrometry with ^{11}B and ^4He ions

The above experimental equipment was used for the Rutherford backscattering spectrometry with ^{11}B and ^4He ions. Targets used were as follows:

Thin targets (5 nm) : Mn, Cu, Ge, Ag, Au, Pb
Thick targets (100 nm) : Mn, Au
Other target : Si single-crystal wafer
(for observation of channeling)

All the targets except for the Si single-crystal wafer were fabricated on Si single-crystal wafers of 10 mm × 10 mm area by means of the vacuum evaporation method. We took the backscattering spectra for these targets in energy ranges of 2-6 MeV for ^{11}B ions and 1-4 MeV for ^4He ions. Voltages supplied to the detector were 100 V and 40 V for ^{11}B and ^4He ions, respectively, which gave the best energy resolutions. The Gaussian curve fitting gave channel numbers at the peaks and their full width at half

maximum (FWHM).

3. Results and discussion

3. 1 Calibration of terminal voltage

First of all, the aluminum thick-target gamma-ray yields were measured as a function of proton energy around the three resonant energies[5] of 632.23, 991.88 and 1213.08 keV. From these yield-curves, values of the deviations $\delta V'$ of the nominal terminal voltages V' from the true voltages V were determined as 0.38, 0.85 and 2.96 kV at nominal voltages of 304.5, 484.8 and 597.5 kV, respectively. For the accelerator, the nominal values of the terminal voltage are obtained by using an electrostatic voltmeter.

Then, we executed a series of "RBS-iterative method" in the nominal voltage range above 597.5 kV. In the procedure, the K-factors of ^{4}He and ^{1}H ions were calculated with the kinematical formula[6] and the energy losses of ^{4}He and ^{1}H ions in the Au target and in the window of the detector were obtained from the values of stopping cross sections taken from Refs. 7) and 8), for ^{4}He and ^{1}H ions, respectively.

Results of the calibration are shown in Fig. 1. Marks '□' show data taken with the "resonance method", and marks '⁎' are those for the "RBS-iterative method". A solid

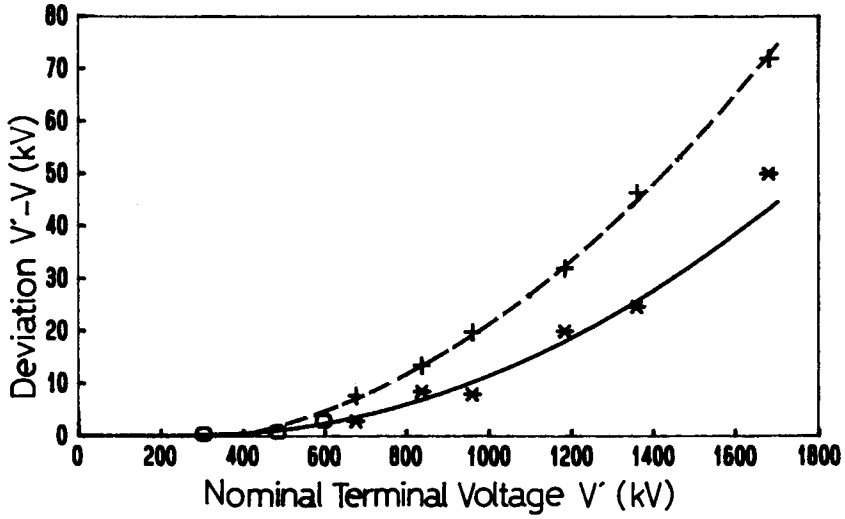

Fig. 1. Calibration of the terminal voltage of TANDETRON. Marks '□' show data taken by the "resonance method", marks '⁎' and '+' show those by the "RBS-iterative method" with and without the corrections for the defects caused by nuclear collision and recombination, respectively. A solid and a dashed line show curves of second degree fitted to the experimental results by the least squares method.

line shows a curve of second degree fitted to the experimental results by the least squares method. A dashed line and marks '+' will be explained below.

In the "RBS-iterative method" mentioned so far, the pulse-height defect (PHD) of the detector has not been taken into account for ^{4}He and ^{1}H. The pulse-height defect has been studied very well for heavy ions such as fission fragments in an energy range between 10 and 100 MeV, but little data are available for ^{4}He and ^{1}H with energies of a few MeV.

Therefore, we have improved empirical equations for the pulse-height defect for heavy ions[9),10)] in order to be applicable to light ions, if necessary, and estimated the affect of the pulse-height defect to the result of the energy calibration by the "RBS-iterative method".

The pulse-height defect E_{PHD} is generally divided into three parts[11)];

$$E_{PHD}=E_w+E_n+E_r \tag{5}$$

where, E_w and E_n are energy losses in the window of the detector and by the nuclear stopping, respectively, and E_r is the defect caused by the recombination of electrons and holes in the detector. As the value of E_w was corrected beforehand in the "RBS-iterative method", it is necessary to estimate only the values of E_n and E_r.

First , the values of $E_n(^4\mathrm{He})$ and $E_n(^1\mathrm{H})$ were obtained by use of Wilkins et al.'s empirical equations[9)], described as,

$$E_n(^4\mathrm{He})=16.55-274.03/\{13.55+0.72(E'-E_w)\} \quad [\mathrm{keV}] \tag{6}$$

$$E_n(^1\mathrm{H}) =7.20-51.84/\{7.20+0.72(E'-E_w)\} \quad [\mathrm{keV}] \tag{7}$$

where, E' is the energy of ions incident on the detector.

Next, the value of the recombination defect E_r was estimated as follows: We have improved the empirical equations by Ogihara et al.[10)] for heavier and more energetic ions, in order to reproduce the observed values of E_r for ^{12}C at 1-8 MeV[12)]. Then, we got the empirical formula for light ions, as given by

$$E_r=(n_{10}/4\pi D_a C)\ln(4D_a t_p/r_o^2)\,(E'-E_w) \quad [\mathrm{MeV}] \tag{8}$$

$$D_a=198\rho^{-0.21}Z^{-0.8}F^{-0.15} \quad [\mathrm{cm^2/s}] \tag{9}$$

$$C=1.66\times10^{11}(E'-E_w)^{0.85}\rho^{0.32}/(A^{1.6}Z^{1.46}) \quad [\mathrm{s/cm^3}] \tag{10}$$

$$t_p=3.25\times10^{-12}\rho^{0.14}Z^{0.5}\{7.5\times10^{14}S(E'-E_w)^{0.85}\}^{0.42}F^{-0.85} \quad [s] \tag{11}$$

$$n_{10}=7.5\times10^8 S \quad [\mathrm{cm^{-1}}] \tag{12}$$

$$F=(d-x)/(1481\times10^{-2}\rho) \quad [\mathrm{V/cm}] \tag{13}$$

$$d=(2\times1481\times10^{-2}\rho V^{0.5})^{0.5} \quad [\mathrm{cm}] \tag{14}$$

where, r_0 is the initial radius of the plasma column [cm], E' the energy of ions incident on the detector [MeV], E_w the energy loss in the window of the detector, ρ the resistivity of the detector [Ωcm], V the detector bias voltage [V], S the total stopping cross section [MeV/(mg/cm^2)], x the distance from the electrode to the position of the maximum density through the passage of ions [cm], and Z, A are the atomic and the mass numbers of the ions. From these equations, E_r(^{4}He) is in the range of 0.36-0.76 keV, and E_r(^{1}H) is in the range of 0.009-0.015 keV in the energy region of the present interest.

Results of the energy calibration which includes the effects of the nuclear stopping and the recombination are shown in Fig. 1 with a dashed line. A solid line shows the result without the corrections, as mentioned above. As seen from the figure, the deviation increases by 75% when the corrections are taken into account. It must be noted that values of E_n and E_r are not observed ones but estimated ones, and they possibly contain uncertainties as much as a few tens percents.

3. 2 Rutherford backscattering spectrometry with ^{11}B and ^{4}He ions

a) Pulse-height defects

The backscattering spectra were taken for 34 pairs of various ions, energies and

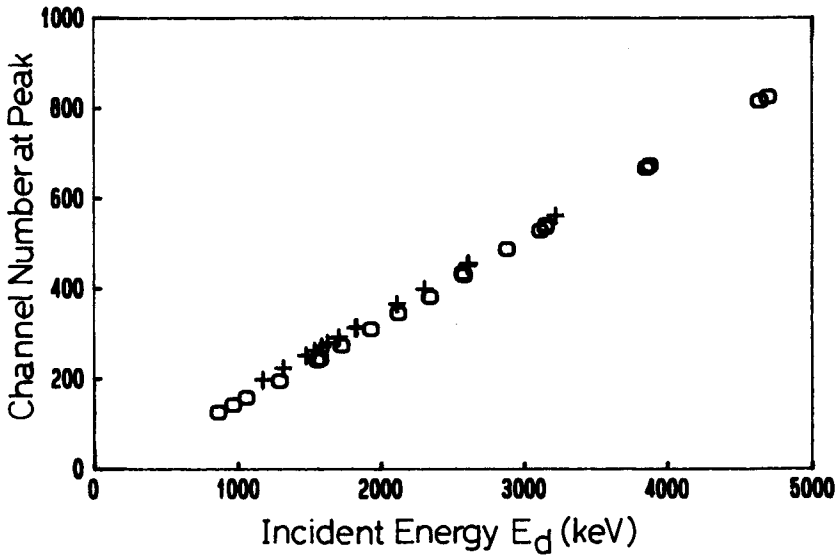

Fig. 2. Pulse-height defects of the semiconductor detector. Channel numbers at peaks are plotted vs. incident energy of ^{11}B and ^{4}He ions. The pulse heights for ^{11}B ions (marks '□') are lower than those for ^{4}He ions (marks '+') at the same incident energy.

targets, and were analyzed to deduce channel numbers at the peaks. In Fig. 2 the obtained channel numbers are shown as a function of incident energy E_d. The values of E_d were obtained by correcting the K-factor, the energy losses in the target E_t and the window of the detector E_w. The values of E_t and E_w were obtained from the stopping cross sections given in Refs. 7) and 13), for ^{4}He and ^{11}B, respectively.

As known from the figure, the pulse heights for the ^{11}B ions are slightly less than those for ^{4}He. This is because of the pulse-height defect of the detector. However, the energy loss in the window of the detector E_w is corrected beforehand in this case, so the observed defects came from differences in the values of the defects by the nuclear stopping E_n and the recombination E_r between ^{11}B and ^{4}He ions. Namely, for the equal values of E_d the pulse height of ^{11}B is lower than that of ^{4}He ions, because the value of E_n+E_r of ^{11}B is larger than that of ^{4}He ions.

b) Sensitivity

Figure 3 compares observed yields of backscattered ions and those expected theoretically[6] per beam fluence of 10μC for Mn and Au targets. The observed yields are slightly less than the expected ones for the reason that the densities of the thin targets prepared by the evaporation method are lower than the respective intrinsic densities.

The backscattered yields of 6 MeV ^{11}B ions are about half of those of 2 MeV ^{4}He

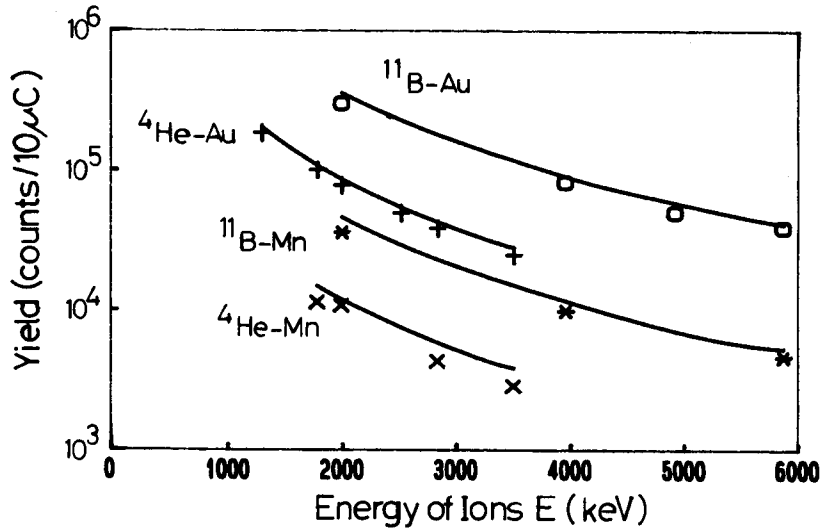

Fig. 3. Yields of backscattered ions per beam fluence of 10 μC vs. energy of ions for several combinations of ^{11}B and ^{4}He ions and Au and Mn targets. Marks and solid lines show the experimental and the expected[6] yields, respectively.

ions. However, we can increase counting rates of backscattered ^{11}B ions by simply increasing a beam current of ^{11}B ions.

c) Energy resolution of system

It is necessary to know first the energy resolutions of the system δE_s in order to apply efficiently the Rutherford backscattering spectrometry to various purposes, because the mass and the depth resolutions depend directly on the energy resolution of the system[6]. The value of δE_s is deduced from the value of FWHM δE for the backscattering spectrum of the thin Au target, by using the following equation:

$$\delta E=\delta E_s+\delta E_t \tag{15}$$

where, δE_t is the energy spread caused by the energy loss of ions in the thin Au target. The value is calculated by use of stopping cross sections taken from Refs. 13) and 7), for ^{11}B and ^4He, respectively. In Fig. 4, δE_s is plotted as a function of E', the energy of ions incident on the detector. A solid and a dashed line show the respective values for ^{11}B and ^4He ions estimated by O'Connor et al[1]. Our experimental values are in good agreement with their estimation for ^4He ions. In the case of ^{11}B ions, the resolution is better for our results than for theirs, but the tendency that the resolution gets worse

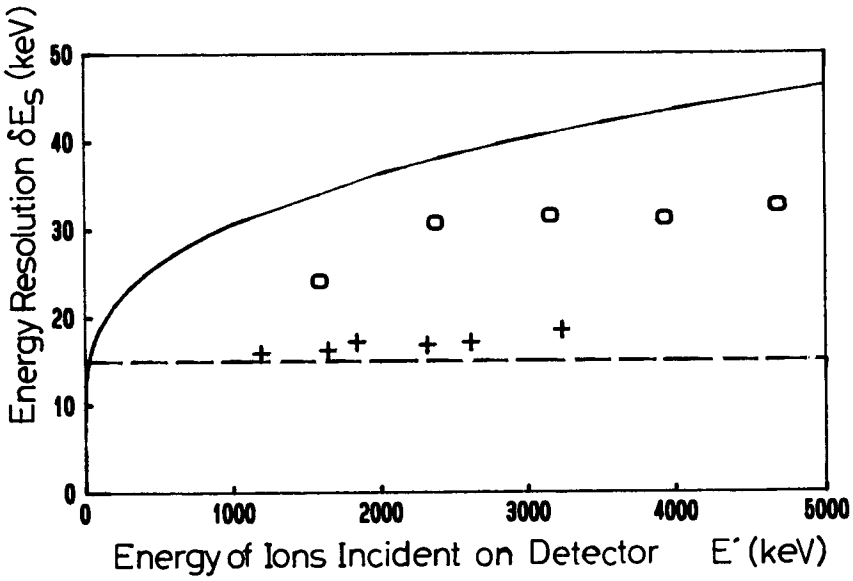

Fig. 4. Energy resolutions of the system δE_s for ^{11}B (marks '□') and ^4He ions (marks '+'). A solid and a dashed line show the estimations by O'Connor et al.[1] for ^{11}B and ^4He ions, respectively.

with increasing energy is in qualitative agreement with their estimation.

d) Mass resolution

The mass resolution of the system δM_s is approximately given by the next equation[14]:

$$\delta M_s = (M^2 \delta E_s) / (4mE) \tag{16}$$

where, M and m are the atomic masses of the target atoms and the incident ions, respectively, E is the energy of the ions incident on the target and δE_s is the energy resolution of the system.

Figure 5 shows the mass resolution obtained for the Au target as a function of energy of ions incident on the target. It is clear that the mass resolution for ^{11}B ions with an energy of 6 MeV is almost 4 times better than that for ^4He ions with an energy of 2 MeV. The feature is displayed in Fig. 6, where (a) and (b) are the spectra for the Cu target of 5 nm thick taken with ^{11}B and ^4He ions, respectively. In the spectrum taken with ^{11}B ions, two isotopes of Cu, ^{63}Cu and ^{65}Cu, are identified unambiguously, but in the spectrum taken with ^4He ions it is difficult to distinguish the respective peaks.

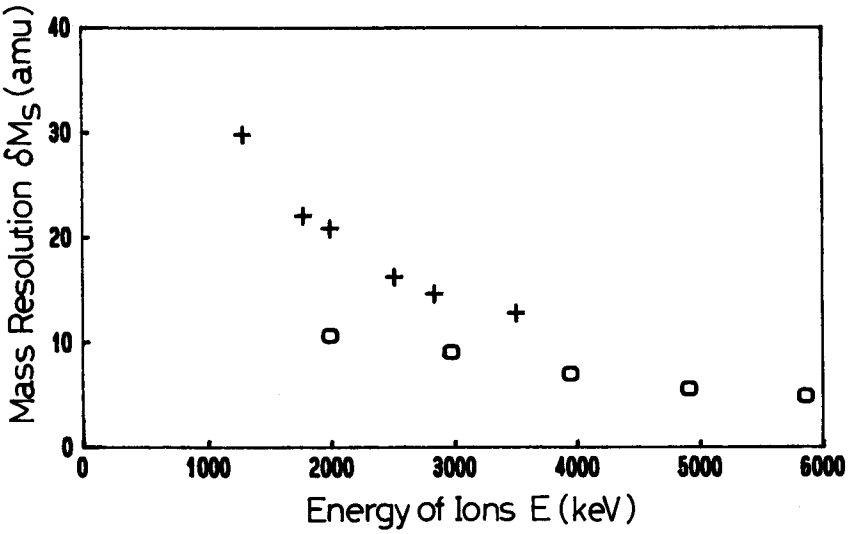

Fig. 5. Mass resolutions of the system δM_s in the case of an Au target for ^{11}B (marks '□') and ^4He ions (marks '+'). δM_s for 6 MeV ^{11}B ions is about 4 times better than that for 2 MeV ^4He ions.

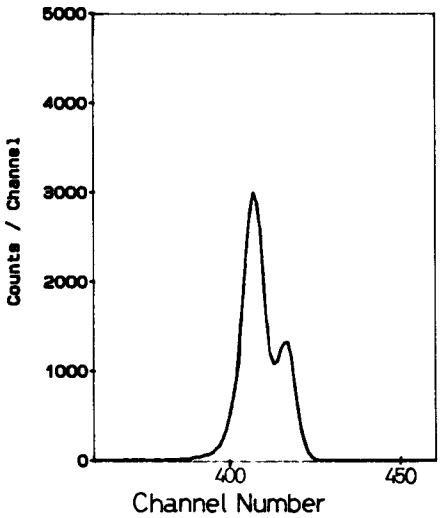

Fig. 6 (a). A pulse height spectrum for a 5 nm Cu target taken with 6 MeV ^{11}B ions. ^{63}Cu and ^{65}Cu are identified unambiguously.

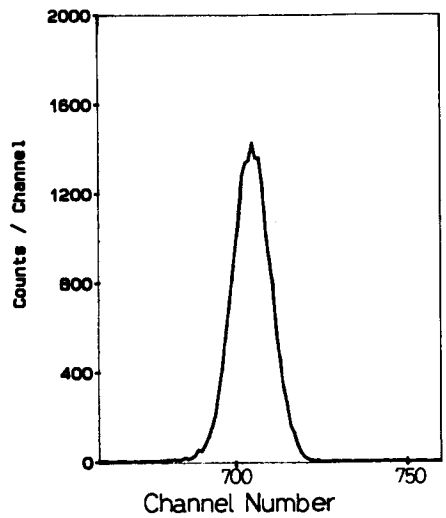

Fig. 6 (b). A pulse height spectrum for a 5 nm Cu target taken with 2 MeV ^{4}He ions. Peaks of ^{63}Cu and ^{65}Cu compose an overlapped single peak.

e) Depth resolution

The depth resolution of the system δT_s is given by the following equation[6]:

$$\delta T_s = \delta E_s / [S] \tag{17}$$

$$[S] = K(\mathrm{d}\dot{E}/\mathrm{d}X)_{in} + (\mathrm{d}E/\mathrm{d}X)_{out}/|\cos\theta| \tag{18}$$

where, δE_s is the energy resolution of the system, K is the K-factor, θ is the scattering angle, and $(\mathrm{d}E/\mathrm{d}X)_{in}$ and $(\mathrm{d}E/\mathrm{d}X)_{out}$ are the stopping cross sections at the energies of incident and outgoing ions, respectively.

Figure 7 shows the obtained depth resolution of the system for the Au target. 6 MeV ^{11}B ions give about 30% better depth resolution than that taken with 2 MeV ^{4}He ions. Figure 8 shows the typical spectra for the Au target 100nm thick taken with 6 MeV ^{11}B and 2 MeV ^{4}He ions. It can be seen from this figure that both the front and the rear edges of the broad peak of Au are steeper for ^{11}B than for ^{4}He ions.

From these results, it is profitable to use 6 MeV ^{11}B ions for the Rutherford backscattering spectrometry, and also from the viewpoint of analysis of the depth profile.

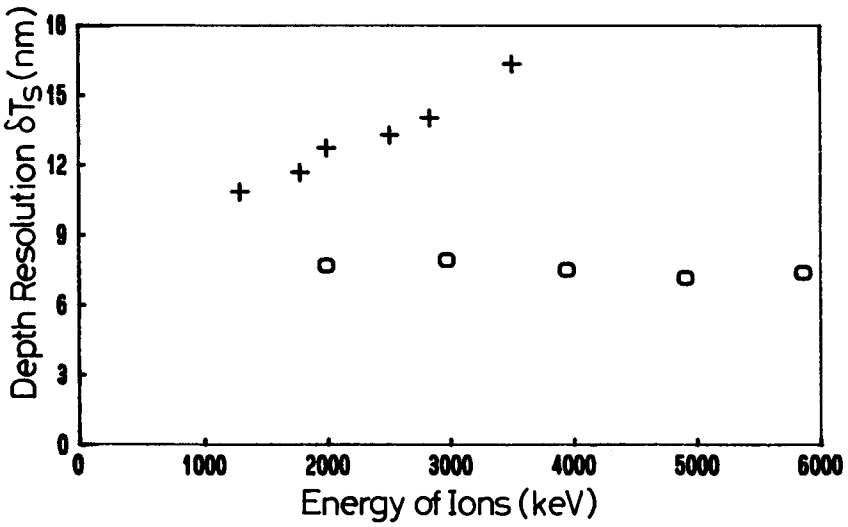

Fig. 7. Depth resolutions of the system δT_s in the case of an Au target for ^{11}B (marks '□') and ^{4}He ions (marks '+'). δT_s for 6 MeV ^{11}B ions is about 30% better than that for 2 MeV ^{4}He ions.

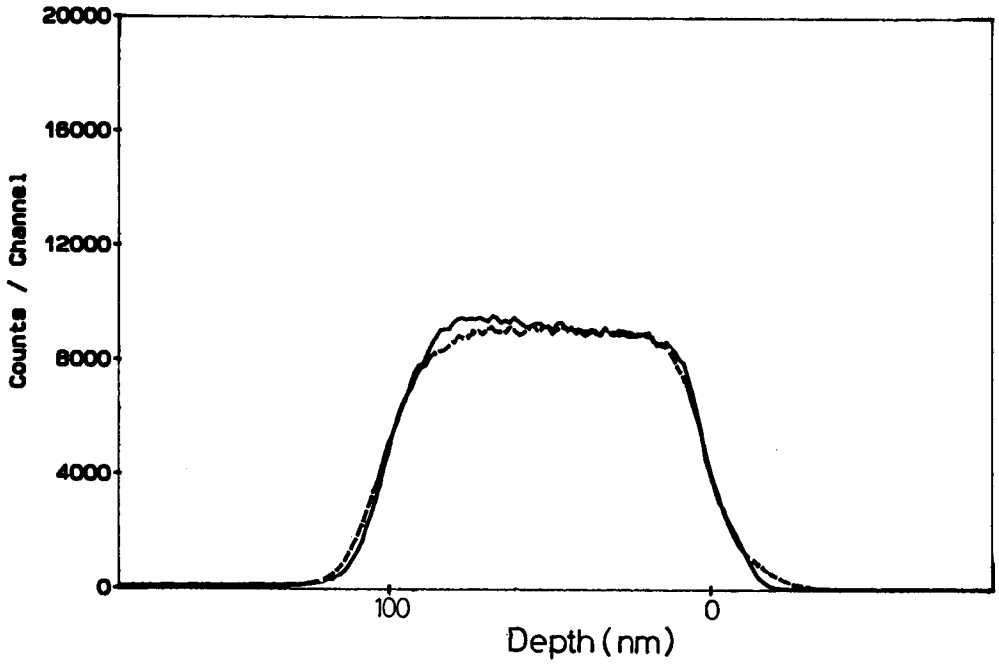

Fig. 8. A comparison of spectra taken with 6 MeV ^{11}B (a solid line) and 2 MeV ^{4}He ions (a dashed line) for an Au target 100 nm thick. The spectrum with ^{11}B ions is more rectangular than that with ^{4}He ions.

f) Channeling minimum yield

We tested the channeling properties of both ions using the silicon single-crystal wafer.

The spectra for aligned and random incidences were taken with ^{11}B and ^{4}He ions. The channeling minimum yields, i. e. (yield for aligned incidence)/(yield for random incidence), were 0.038 and 0.057 for ^{11}B and ^{4}He ions, respectively. Thus, the channeling minimum yield with 6 MeV ^{11}B ions is 33% better than that with 2 MeV ^{4}He ions. The result can be qualitatively understood from the fact that the heavy and energetic ions go through the axis of the crystal farther than the light and low energy ions.

g) Radiation damage of semiconductor detector

Spurious peaks appeared in the spectra taken with ^{11}B ions after heavy irradiation. Figure 9 shows an example of the spectra. The spectra taken with ^{4}He and ^{1}H ions showed no spurious peak. Therefore, the spurious peaks were caused by radiation damage located close to the entrance of the depletion layer.

The radiation damage of a semiconductor detector can be induced at a relatively low fluence by heavy ions when compared with light ions such as ^{1}H and ^{4}He ions[11].

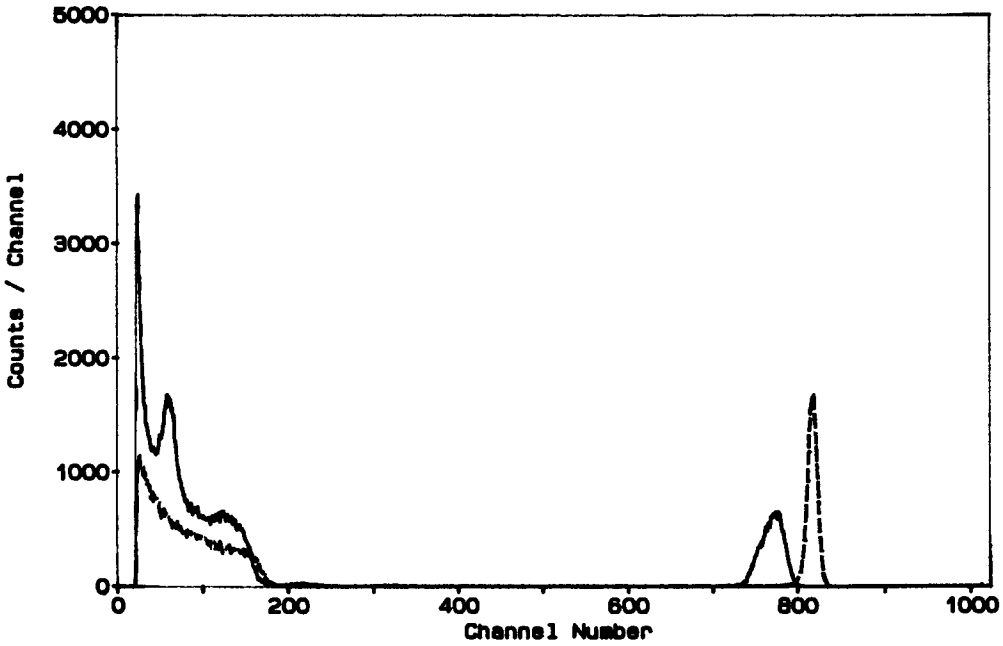

Fig. 9. Examples of spectra taken with 6 MeV ^{11}B ions before and after heavy irradiation (a dashed and a solid line, respectively). An energy resolution got worse and a spurious peak appeared on the broad pedestal for Si. The observation reflects the radiation damage in the detector.

Therefore, one must pay sufficient attention to avoid exposing the detector to unnecessary heavy-ion beams.

4. Conclusions

True terminal voltages of "TANDETRON" are lower than the corresponding nominal values. The deviation depends on the terminal voltage quadratically, and extends to 44 kV at a maximum nominal voltage of 1.7 MV. When the pulse-height defects caused by nuclear collision and recombination are taken into account, the deviation increases, and becomes as large as 74 kV at a maximum nominal voltage of 1.7 MV.

Backscattering spectra improve in the mass resolution, the depth resolution and the channeling minimum yield when 6 MeV ^{11}B ions are used instead of 2 MeV ^{4}He ions, which have been used commonly. However, we must pay attention in order not to cause radiation damage by irradiating heavy ions to the detector.

Acknowledgment

The authors would like to express their thanks to Dr. M. Tomita, Mr. K. Norisawa, Mr. T. Ohdaira, Mr. H. Matsushita, Mr. T. Sato, Mr. N. Sakura and Mr. A. Takashima for their helpful advice and experimental support.

References

1) D. J. O'Connor and TAN Chunyu; Nucl. Instr. and Meth. **B36**, 178 (1989)
2) A. Chevarier, N. Chevarier, M. Stern, D. Lamouche, P. Clechet, J. R. Martin and P. Person; Nucl. Instr. and Meth. **B13**, 207 (1986)
3) Marcus H. Mendenhall and Robert A. Weller; Nucl. Instr. and Meth. **B47**, 193 (1990)
4) M. Östling, C. S. Petersson, P. Johansson, A. Wikstrom and G. Possnert; Nucl. Instr. and Meth. **B15**, 729 (1986)
5) P. M. Endt and C. Vanderleun; Nucl. Phys. **A310**, 235 (1978)
6) L. C. Feldman and J. W. Mayer; "Fundamentals of Surface and Thin Film Analysis", North-Holland, New York, pp. 13-68 (1986)
7) J. F. Ziegler and W. K. Chu; Atom. Data and Nucl. Data Tables **13**, 463 (1974)
8) J. F. Janni; Atom. Data and Nucl. Data Tables **27**, 341 (1989)
9) B. D. Wilkins, M. J. Fluss, L. B. Kaufmann, C. E. Gross and E. P. Steinberg; Nucl. Instr. and Meth. **92**, 381 (1971)
10) M. Ogihara, Y. Nagashima, W. Galster and T. Mikumo; Nucl. Instr. and Meth. **A251**, 313 (1986)
11) G. F. Knoll; "Radiation Detection and Measurement", John Wiley & Sons, New York, pp. 371-372 (1989)
12) G. Sato, M. Saito, K. Iwasawa, N. Imanishi and F. Fukuzawa; to be published

13) J. F. Ziegler, J. P. Biersack and U. Littmark ; "The Stopping and Ranges of Ions in Solids, Vol. 1 of The Stopping and Ranges of Ions in Matter", Pergamon Press, New York, p. 209 (1985)
14) P. Eichinger and H. Ryssel ; "Ion Implantation Techniques", Edited by H. Ryssel and H. Glawishnig, Springer-Verlag, Berlin, p. 286 (1982)